## PAPER

Check for updates

# Integrated pyrolysis of pine needles and cashewnut shells: optimizing process conditions for the production of renewable fuel and value-added chemicals

Sowkhya Naidu,[a] Sivasankar Kakku,[a] Ranjeet Kumar Mishra, [ID] *[b] Prathap Somu,[a] Jyeshtharaj Joshi,[c] Chiranjeevi Thota, [ID] [d] Sathrugnan Karthikeyan[f] and Abhishek Sharma*[aeg]

The sustainable conversion of lignocellulosic residues into renewable fuels and chemicals is vital to advancing a circular bioeconomy. This study presents a dual-scale thermochemical framework for the valorisation of pine needles (PN) and cashewnut shells (CNS) through integrated analytical and pilot-scale pyrolysis. Analytical pyrolysis using Py-GC/MS was employed to evaluate the temperature-dependent formation of bio-volatiles between 400 and 800 °C, revealing that 500 °C yielded the highest fraction of desirable compounds. PN generated aromatic-rich volatiles suitable for advanced fuel formulations, while cashewnut shells produced phenolic-rich vapours with applications in the renewable chemicals sector. The scale-up experiments conducted in a semi-pilot rotary kiln reactor confirmed the reproducibility of product yields and compositional trends observed at the laboratory scale. The maximum pyrolysis oil yields reached 40% for PN and 33% for CNS, while char and gas yields varied according to lignocellulosic composition. The elemental analysis indicated superior fuel quality for PN-derived bio-oil (higher heating value (HHV) = 35.08 MJ kg$^{-1}$, O/C = 0.23) compared with CNS oil (HHV = 28.14 MJ kg$^{-1}$, O/C = 0.43). Furthermore, biochars exhibited porous morphologies, indicating potential for environmental applications. This dual-scale methodology effectively bridges mechanistic understanding with process scalability, enabling tailored valorisation routes for underutilised biomass residues.

## 1. Introduction

Fossil fuels (including coal, oil, and natural gas) account for more than 75% of worldwide greenhouse gas emissions and are the primary factors driving climate change. To meet global climate goals, industries must reduce global emissions by 50% by 2030 and achieve net zero by 2050. Shifting towards renewable energy sources, such as solar, wind, and waste, is crucial. While fossil fuels account for 80% of the global energy supply, renewable sources comprise 29% of global electricity generation.[1] Biomass has attracted considerable global interest as a versatile feedstock for producing energy and chemicals, due to its abundance, carbon neutrality, and capacity to transform waste into valuable resources.[2] Recent advancements in biomass pyrolysis, domestically and globally, underscore its potential for generating bio-oil, biochar, and syngas. Current research focuses on improving quality and scalability through process intensification, feedstock diversification, and product enhancement. Global challenges, including fuel efficiency, oil price instability, energy security, and climate change, underscore the need for change. Fossil fuels meet about 90% of energy needs, but experts expect renewable resources to provide 50% by 2040.[3,4] Rising oil prices and climate concerns drive increased attention to biomass-based biofuels as a sustainable alternative.[5] In India, where diverse agro-forestry residues are readily available, and globally, where lignocellulosic conversion has been extensively explored, pyrolysis has emerged as a pivotal pathway for reducing fossil fuel dependence while

[a]*Waste to Resources Laboratory, Department of Biotechnology and Chemical Engineering, Manipal University Jaipur, Rajasthan, 303007 India. E-mail: abhishek. sharma@jaipur.manipal.edu*

[b]*Department of Chemical Engineering, Manipal Institute of Technology, Manipal Academy of Higher Education, Manipal, Karnataka 576104, India. E-mail: ranjeet. mishra@manipal.edu*

[c]*Department of Chemical Engineering, Institute of Chemical Technology, Mumbai, Maharashtra 400019, India*

[d]*Corporate Research & Development Centre, Bharat Petroleum Corporation Limited, Greater Noida, UP, 201306, India*

[e]*Chemical & Environmental Engineering, School of Engineering, RMIT University, Melbourne, Victoria 3000, Australia*

[f]*Frontier Laboratories Ltd, 4-16-20 Saikon, Koriyama, Fukushima 963-8862, Japan*

[g]*Department of Chemical Engineering, BITS Pilani K. K. Birla Goa Campus, Goa 403726, India*

supporting the circular bioeconomy. However, competing uses of biomass for energy and other sectors such as agriculture and forestry pose challenges, necessitating integrated strategies for sustainable biomass use.[6]

Biomass pyrolysis in rotary kiln reactors has garnered significant research attention due to their capability for continuous thermal conversion of diverse lignocellulosic feedstocks into bio-oil, biochar, and syngas. Rotary kilns offer key advantages, including controlled residence time, uniform heat transfer enabled by gradual rotation, and high tolerance to varying biomass forms without extensive pretreatment, making them superior to fixed-bed and fluidized-bed systems for many applications.[7] Recent computational advances, especially the integration of computational fluid dynamics (CFD) with discrete element modelling (CFD-DEM), have strengthened mechanistic understanding by accurately simulating heat transfer, particle flow, and conversion pathways in rotary drums, thereby supporting the transition from analytical-scale assessments to pilot-scale reactor validation.[8] Pilot-scale investigations have demonstrated the capability of rotary kilns to produce biochar with tailored physicochemical properties for soil and environmental applications, along with bio-oils enriched in phenolic and aromatic compounds, which are suitable for energy and chemical use.[7,9] Semi-pilot co-pyrolysis of groundnut shells with plastics (LDPE, HDPE, PP) at 500 °C achieved oil yields up to 49% (GS/HDPE 40 : 60). Gas yields of 36% (GS/LDPE 40 : 60), exhibiting synergistic enhancements in heating value (25–43 MJ kg$^{-1}$) and increased aromatic content (45%) with reduced phenolics.[10] Additional research using continuous semi-pilot auger reactors across a temperature range of 400–700 °C further optimised product quality and yield.[11] Emerging innovations, such as two-stage rotary kilns with internal baffles, have improved syngas yield, reduced tar formation, and enhanced conversion efficiency, thereby expanding the industrial potential.[12] Nevertheless, linking molecular-level pyrolysis chemistry with reactor-scale behaviour remains a critical challenge, underscoring the need for integrated analytical and pilot-scale research to support industrial-scale deployment.[7,13]

Two biomass residues, forestry residues (PN) and agricultural residues (CNS), were used in this study for bioenergy production. Indian states, such as Uttarakhand, have a substantial biomass utilisation potential due to their extensive forest coverage, which covers 71% of their area (37 999 km$^2$).[14,15] *Pinus roxburghii* (chir pine) is a promising biodiesel feedstock among its forest resources. The state's pine forests, which span approximately 3.43 lakh hectares, produce more than 20.58 lakh tons of dried biomass annually, primarily from PN. The Uttarakhand Forest Department has authorised the collection of only 40% of this biomass (8.23 lakh tons) due to logistical constraints.[16,17] The slow decomposition of PN causes them to accumulate on the forest floor, forming a dense layer that poses fire hazards and inhibits grass growth essential for cattle grazing.[18] Further, the accumulation of PN exacerbates large-scale forest fires, leading to ecological devastation and air pollution. The conversion of PN into bio-oil and biochar is a sustainable solution using pyrolysis, among all

thermochemical conversion processes. In 2024, the valuation of the cashew market in India was estimated at USD 2.4 billion, with expectations of a compound annual growth rate (CAGR) of 3.8%, projected to reach USD 2.9 billion by 2029. This industry is projected to produce over 0.8 million tons across 0.7 million hectares, contributing USD 0.47 billion in foreign exchange and generating jobs for 1.5 million individuals.[19] Maharashtra, Andhra Pradesh, Odisha, Karnataka, Chhattisgarh, Andamans, Northeast, and Tamil Nadu are other major producers.[20] However, improper shell disposal pollutes land and water, and open burning emits hazardous fumes[21] cashewnut shell liquid (CNSL) has a high calorific value (40 MJ kg$^{-1}$).[22] Lower ash content (0.01%), and moisture content of 3–3.5 wt%, making it suitable for industrial uses like friction linings, paints, varnishes, adhesives, polymers, bactericides, insecticides, and surface-active agents.[23] The cashew nutshell possesses a high calorific value ranging from 16 to 22 MJ kg$^{-1}$ [24] and, using cashew shells as solid biofuels offers an effective management alternative.

Various technologies are available for turning waste residues into valuable products. Among them, pyrolysis is one of the most prominent options that yields products in various states, such as solid, gas, and liquid, making it a key technology for waste valorisation and sustainable energy production. Pyrolysis is again divided into two major types: analytical and applied pyrolysis. Py-GC/MS is an advanced analytical technique for analysing volatile and high-boiling-point chemicals.[25,26] It is widely used for qualitative and semi-quantitative studies of biomass pyrolysis products, although equipment limitations and product complexity limit volatile species identification.[27] Recently developed Py-GC/MS can accurately detect pyrolysis products by correlating chromatograms with the NIST library under different conditions. Several studies have shown the potential applications of Py-GC/MS.[23] investigated the fast pyrolysis behaviour of biomass with high ash and nitrogen content using TG-FTIR and Py-GC/MS.[28] It analyses thermal decomposition, volatile product distribution, and gas-phase chemistry, highlighting how ash and nitrogen influence bio-oil composition, gas emissions, and pyrolysis efficiency. It offers insights for optimising biomass conversion processes. Huang *et al.* (2020)[24] investigate the pyrolysis of various parts of water hyacinth biomass using TG-FTIR and Py-GC/MS to assess the bioenergy potential, gas emissions, and by-product composition. It highlights variations in thermal decomposition, volatile formation, and emission profiles, providing insights into optimizing bio-oil yield and minimizing environmental impact during biomass conversion.[29] Mishra *et al.* (2020) investigate the thermal characteristics, kinetics, and rapid pyrolysis of *cynodon dactylon* grass through Py-GC/MS and Py-FTIR techniques. It analyses decomposition pathways, volatile products, and reaction kinetics, providing insights into bio-oil composition, gas emissions, and optimal pyrolysis conditions for maximizing biofuel production while minimizing environmental impact.[30] Kaur *et al.* (2022) investigate the pyrolysis behaviour of eucalyptus, mentha, and palmarosa biomass using Py-GC/MS to analyse volatile products and thermal decomposition characteristics. It identifies key bio-oil components,

**Table 1** Comparative analysis of biomass pyrolysis approaches

| Feature | Conventional pyrolysis methods | Proposed dual-scale pyrolysis approach |
|---|---|---|
| Pyrolysis scale | Laboratory-scale | Analytical (Py-GC/MS) and pilot-scale (rotary kiln) |
| Feedstock utilization | Limited to specific feedstocks | Diverse feedstocks (PN and CNS) |
| Product selectivity | General distribution | Targeted bio-oil for energy and chemical applications |
| Mechanistic insights | Limited molecular-level analysis | Detailed mechanistic understanding *via* Py-GC/MS |
| Scalability validation | Often unverified | Pilot-scale validation ensures product consistency |
| Process integration | Standalone processes | Integrated analytical and operational scales |
| Innovation | Established methods | Novel dual-scale strategy bridging lab and pilot scales |

including phenolics, ketones, and hydrocarbons, optimizing pyrolysis conditions for maximum biofuel yield while evaluating the influence of feedstock composition on product distribution.[31] Furthermore, the application of pyrolysis to biomass has also been explored and reported in the literature. The pyrolysis process is conducted using different feedstocks, reactor types and temperatures to determine product yields and chemical compositions. Saleh Al Arni (2018) studied slow and fast pyrolysis for biomass conversion into fuel, analysing product distribution, reaction kinetics, and thermal behaviour.[32] Slow pyrolysis favours biochar production, while fast pyrolysis enhances bio-oil yield. The research highlights optimal conditions, feedstock influence, and process efficiencies for improving biofuel quality and sustainable energy applications.[33] Mishra *et al.* (2020) examine the pyrolysis kinetics and thermal decomposition behaviour of *Samanea saman* seeds for renewable fuel production.[29] Using kinetic modelling and pyrolysis analysis, it evaluates reaction mechanisms, bio-oil composition, and optimal process conditions, providing insights into maximizing fuel yield and improving the efficiency of biomass-to-energy conversion.[34] Van Nguyen *et al.* (2019) investigate the enhancement of bio-oil characteristics by co-pyrolyzing pine sawdust with waste polystyrene foam.[30] The study assesses the synergistic effects on product yield, chemical composition, and fuel quality, revealing an increased hydrocarbon content, lower levels of oxygenates, and improved energy potential for sustainable biofuel applications.[35] Varma *et al.* (2019) investigated the pyrolysis of wood sawdust, focusing on the effects of process parameters on product yield and characterization.[31] The study analyzed the influence of temperature, heating rate, and residence time on bio-oil, biochar, and gas production, providing insights into optimizing operating conditions for improved fuel quality and sustainable biomass conversion.[36] Despite extensive research on biomass pyrolysis, significant gaps remain in optimising pyrolysis conditions for underutilised feedstocks such as PN and CNS. Previous works have largely focused on single biomass systems, overlooking the synergistic effects between forestry and agricultural residues. Additionally, comparative analysis linking molecular-level decomposition (*via* Py-GC/MS) with pilot-scale reactor validation is scarce, which limits the translation of laboratory insights into industrial applications. The influence of lignin-to-cellulose ratios on pyrolysis oil selectivity, product quality, and char functionality has also not been systematically optimised. Furthermore, few studies correlate analytical pyrolysis profiles

with real reactor performance, leaving uncertainties in scale-up efficiency and product reproducibility. The role of biochar morphology and physicochemical characteristics in determining post-pyrolysis applications is similarly underexplored. Addressing these gaps through an integrated dual-scale pyrolysis framework provides a new direction for achieving efficient biomass valorization and sustainable circular bioeconomy solutions.

This study presents a novel dual-scale pyrolysis approach to address these gaps, combining analytical-scale Py-GC/MS investigations with semi-pilot rotary kiln reactor experiments. This strategy enables synergy of volatile formation, scale-up validation of product yields, and biochar characterization for potential environmental uses. By differentiating product selectivity aromatic-rich bio-oil from PN for energy applications and phenolic-rich bio-oil from CNS for chemical industries, this work emphasizes feedstock-specific behaviour and operational scale in achieving targeted valorisation. This integrated framework not only strengthens the scientific understanding of biomass conversion pathways but also establishes a scalable route for converting underutilized residues into value-added biofuels and chemicals, advancing circular bio-economy objectives. This study aligns with SDG 7 (affordable and clean energy), SDG 12 (responsible consumption and production), SDG 13 (climate action), SDG 14 (life below water) and SDG 15 (life on land) by converting biomass waste into renewable bio-oil and biochar through sustainable pyrolysis, thereby promoting circular resource utilisation and reducing dependence on fossil fuels. This work contributes to SDG 7 by generating renewable bio-oil and biochar from biomass residues as alternatives to fossil-based energy sources. It supports SDG 6 through biochar-enabled water remediation. By reducing open burning and emissions, it advances SDG 13 (climate action), while also protecting aquatic systems (SDG 14) and mitigating land degradation and forest-fire risks (SDG 15). Table 1 shows the comparative analysis of biomass pyrolysis approaches.

## 2. Materials and methods

### 2.1. Sample collection and preparations

PN were collected from Uttarakhand, while cashew nut shells (CNS) were sourced from Mumbai, Maharashtra, India. The collected biomass was dried in the sun and subsequently placed in a hot air oven to uniformly eliminate moisture content. Next, the oven-dried samples were ground using a lab mixer grinder to a particle size between 1 and 4 mm (to be utilised in the rotary

kiln reactor). Following this, a mill was employed to further reduce the particle size to within the range of 0.1 mm to 0.5 mm (for Py-GC/MS analysis). The processed biomass was stored in airtight plastic bags to avoid moisture intake for future experiments.

## 2.2. Physicochemical characterization of biomass

The feedstocks underwent chemical and physical characterization to assess their suitability for subsequent processing. Proximate analysis was performed according to the ASTM D5142 and D1762-84 methods, which measured volatile matter, moisture content, fixed carbon, and ash content. Furthermore, elemental analysis was performed using an Elemental Analyser (Thermo Flash Smart, Thermo Fisher Scientific), in accordance with ASTM D5373 standards. The oxygen percentage was calculated by difference, and the HHV of the fuel was determined using Dulong's formula[37] (eqn (1)). The bulk density was assessed using a digital balance and a measuring cylinder. Furthermore, the biochemical composition of the samples, including hemicellulose, cellulose, and lignin, was examined through wet chemistry techniques.

$$\text{HHV (MJ kg}^{-1}) = 0.3383 \times C + 1.443 \times H - 0.1804 \\ \times O + 0.0942 \times S \tag{1}$$

## 2.3. Thermal stability and FTIR analysis

Thermogravimetric analysis (TGA) of the feedstock was conducted using the NETZSCH model STA 449 F3 Jupiter® under a controlled nitrogen atmosphere to prevent oxidation. A purge gas flow rate of 50 mL min$^{-1}$ ensured a controlled environment, while a protective gas flow rate of 20 mL min$^{-1}$ was kept throughout the test. The sample (8 mg) was placed in the crucible, and the heating process started from room temperature to 900 °C at 10 °C min$^{-1}$. Fourier Transform Infrared (FTIR) spectroscopy was employed to identify the functional groups present in biomass and plastic materials across samples with varying ratios. A small portion of each sample was thoroughly blended with oven-dried potassium bromide (KBr) powder in a 1 : 100 ratio and placed into the sample holder. The spectra were recorded over the wavenumber range of 400–4000 cm$^{-1}$, using a scanning rate of 40 scans per second and a resolution step size of 4 cm$^{-1}$.

## 2.4. Experimental set-up

The pyrolysis experiment was performed using two different pyrolysis processes, known as (a) analytical (Py-GC/MS analysis) and (b) applied pyrolysis. Analytical pyrolysis studies the decomposition mechanisms, kinetics, and product composition at a smaller scale using advanced analytical techniques, such as Py-GC/MS, Py-FTIR, and TGA-FTIR. Furthermore, applied pyrolysis focuses on the practical implementation of producing fuels, chemicals, and materials on a larger scale using commercial reactors, such as rotary kiln reactors. To be more precise, analytical pyrolysis enhances scientific understanding at a smaller scale, whereas applied pyrolysis translates this knowledge into real-world applications for sustainable energy and material recovery.

**2.4.1. Py-GC/MS study.** The analytical pyrolysis of PN and CNS was performed using a Py-GC/MS analyzer. Pyrolysis-Gas Chromatography-Mass Spectrometry (Py-GC/MS) (Fig. 1(a)) was used to analyse the volatile products generated during the fast pyrolysis of biomass at 400, 500, 600, 700, and 800 °C with a heating rate of 600 °C min$^{-1}$. The desired amount of sample (1–1.5 mg) was placed into the sample holder, and the top end of the holder was sealed with glass wool to prevent the sample from overflowing. The sample was measured in an electronic balance with an accuracy of 0.001 µg. Each run was processed thrice in a pyrolysis unit (Frontier Laboratories Ltd, PY-3030D, Japan) with a residence time of 0.3 min at each temperature. The hot volatiles generated during pyrolysis were analysed in GC/MS (Shimadzu-QP2020). A high-purity helium gas served as the carrier gas with a split ratio of 1 : 50. An Rxi-5Sil MS capillary column (30 m × 0.25 mm × 0.25 µm) facilitated chromatographic separation. The GC was initially programmed at 40 °C, held for 2 minutes, then increased to 300 °C at a heating rate of 20 °C min$^{-1}$, while the injector temperature was maintained at 300 °C. The system acquired mass spectra in electron ionization (EI) mode at 70 eV, and scanning ($m/z$) values from 29 to 550. Finally, each peak was matched with the NIST MS library to determine the composition of hot vapours. The schematic layout of the Py-GC/MS setup is listed in Fig. 1(a).

**2.4.2. Rotary kiln reactor.** The applied pyrolysis of PN and CNS was carried out in a semi-pilot scale rotary kiln reactor. The reactor consisted of a horizontal stainless steel (SS-304) tube of 1360 mm length, 355 mm outer diameter and 3 mm wall thickness with a processing capacity of 50 kg day$^{-1}$. The reactor drum was externally heated by three-zone heaters, each with a power rating of 9 kW. The reactor included a heated vessel with a 2 kW heater to maintain the temperature of volatile compounds between 150 °C and 350 °C, ensuring controlled vapour handling. The setup consisted of three oil collection vessels and a series of three condensers, designed to capture heavier fractions efficiently. Each condenser operated at a different temperature to condense the hot vaporers into liquid. A gas flowmeter was used to measure the non-condensable gases (NCG) and pass them through a compressed knitted stainless steel mesh scrubber, which is installed at the end of the vapor pipeline to ensure effective gas purification. The pyrolysis experiment was performed at 500 °C with a heating rate of 50 °C min$^{-1}$. The holding time was maintained at 120 min for complete pyrolysis, with 5 kg of feed material introduced into the reactor. The rotary kiln speed was kept at 1 rpm throughout the test in an oxygen-deficient environment. The heating vessel (V1) produced no oil fraction, whereas the first condenser vessel (V2) yielded the pyrolytic oil. The pyrolytic oil in the liquid product was separated. After the kiln reached room temperature (30 °C), char was extracted from the rotary drum through natural cooling. The yields of liquid, biochar, and syngas were determined using eqn (2), (3) and (4), respectively. The yield of non-condensable gas (NCG) was calculated by subtracting the NCG yield from the total yield, thereby ensuring a mass balance closure. To maintain consistency and reproducibility in the results, all experiments were conducted in triplicate. Eqn (2)–(5) were employed to calculate the
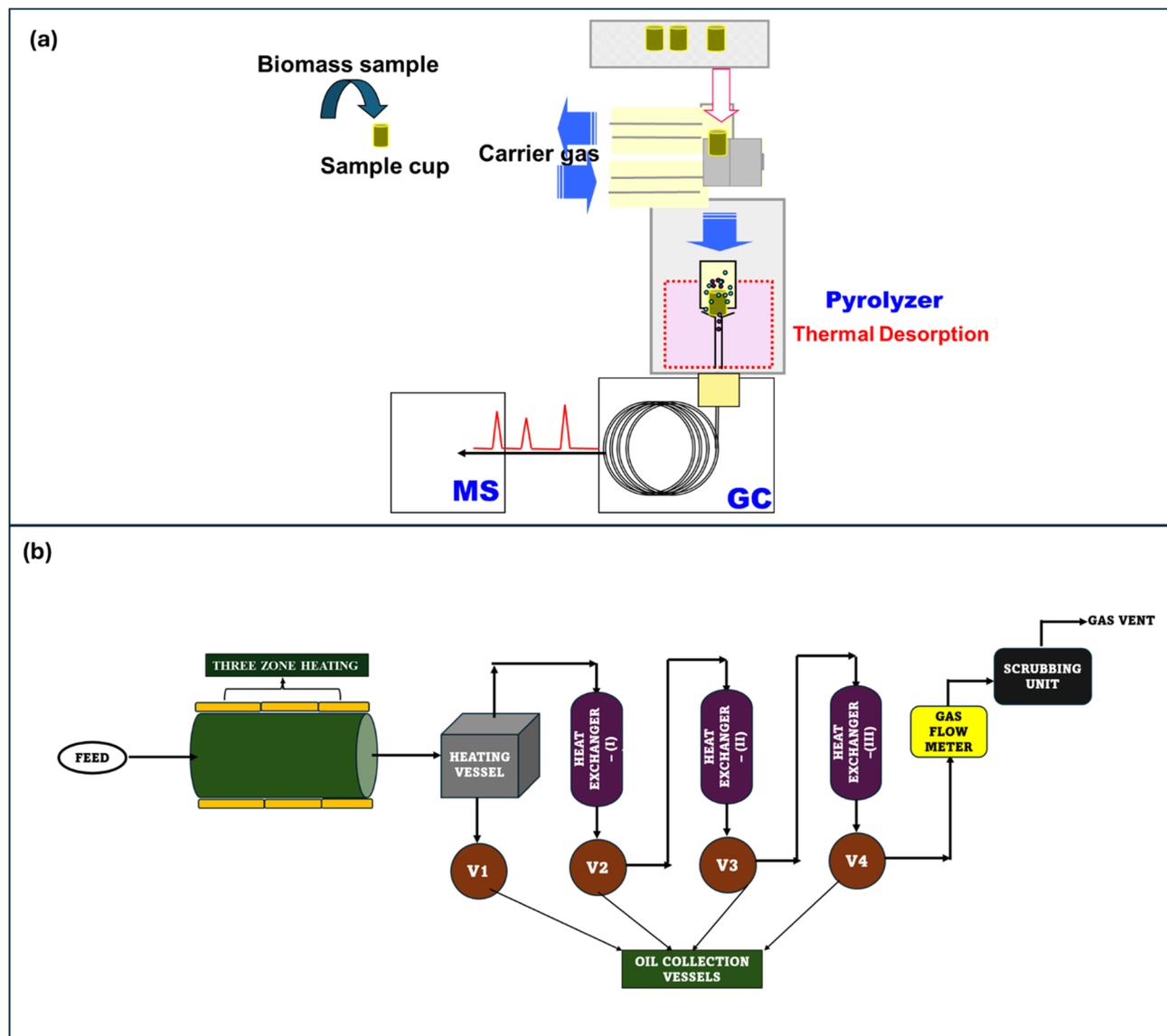
**Fig. 1** Schematic layout of (a) Pyrolysis-Gas Chromatography-Mass Spectrometry (PY-GC/MS) and (b) semi-pilot rotary kiln reactor system.

weight percentages of oil, char, and gas products. A schematic representation of the experimental setup is illustrated in Fig. 1(b).

$$Feed = oil + char + gas \tag{2}$$

$$Oil\ (wt\%) = \frac{weight\ of\ oil}{feed} \times 100 \tag{3}$$

$$Char\ (wt\%) = \frac{weight\ of\ char}{feed} \times 100 \tag{4}$$

$$Gas(wt\%) =$$

$$\frac{weight\ of\ gas = (feed - weight\ of\ oil - weight\ of\ char)}{feed} \times 100 \tag{5}$$

$$Ratio\ of\ \frac{H}{C} = \frac{\left(\dfrac{H\%}{Mol.\ wt\ of\ H}\right)}{\left(\dfrac{C\%}{Mol.\ wt\ of\ C}\right)} \tag{6}$$

$$Ratio\ of\ \frac{O}{C} = \frac{\left(\dfrac{O\%}{Mol.\ wt\ of\ O}\right)}{\left(\dfrac{C\%}{Mol.\ wt\ of\ C}\right)} \tag{7}$$

### 2.5. Physicochemical characterisation of pyrolysis oil

The bio-oil exhibited a black colour and a semi-liquid consistency. The HHV and elemental analysis of pyrolysis oil were performed using the method listed in Section 2.2. Further, the moisture content was measured using a Karl Fischer Titrator

(Model 1760, ESICO). The chemical composition of bio-oil fractions was determined using a Gas Chromatograph-Mass Spectrometry (GC/MS) analyzer (Shimadzu, Model: QP2020) equipped with a Rxi-5 MS column (30 m × 0.25 mm ID, 0.25 µm film thickness). The GC oven temperature program began at 50 °C, lasted for 2 minutes, and was subsequently increased at a rate of 6 °C min$^{-1}$ to 90 °C, followed by a further increase at 6 °C min$^{-1}$ to 120 °C. The temperature was then raised at 8 °C min$^{-1}$ to 250 °C and finally at 10 °C min$^{-1}$ to 280 °C. The injection temperature was maintained at 250 °C, with helium as the carrier gas at a flow rate of 1.18 mL min$^{-1}$ and a split ratio of 15. The MS ion source and interface temperatures were set to 230 °C and 250 °C, respectively. For sample preparation, 200 mg of pyrolysis oil was dissolved in 10 mL of solvent (either acetone or hexane), dehydrated with 4 g of anhydrous sodium sulfate, and subsequently filtered through a 0.22 µm syringe filter. The filtered solution was then injected into the GC/MS in triplicate for analysis. In the current study, GC/MS peak areas were normalised by averaging the areas of each compound from triplicate injections of every sample. The Relative Standard Deviation (RSD) values for the triplicate injections were below 15%. All GC/MS analyses were performed on the same day (intraday), and the normalisation of GC/MS areas was carried out externally rather than using an internal standard mixture.

### 2.6. Characterisation of biochar

The biochar was pulverised into a fine powder with a lab cum mixture grinder. The pH of the biochar was determined by dissolving 1 g of moisture-free biochar into 50 mL of distilled water. The solution was mixed for 4–5 h for uniform mixing using a magnetic stirrer. The pH meter (Toshcon Industries) was calibrated using buffer solutions with pH values of 4, 7, and 9. Furthermore, the surface morphology and composition of the pyrolysis char were determined using a Scanning Electron Microscope (SEM, JEOL JSM-7610 F-Plus).

## 3. Results and discussions

### 3.1. Physicochemical characterisation of biomass

The physicochemical characteristics of PN and CNS were evaluated in comparison to the pyrolysis properties of groundnut-shell and woodsawdust,[38] as shown in Table 2. Proximate analysis for both feedstocks indicated that the moisture levels in PN (3.2 wt%) and CNS (1.5 wt%) were significantly below the 10% threshold, making them appropriate for pyrolysis. However, the moisture content of a feedstock is a critical factor for pyrolysis suitability, independent of drying duration. The analysis revealed that PN contained 2.20 wt% ash and CNS had 4.30 wt% ash, while PN measured 79.13 wt% volatile matter and CNS measured 77.10 wt% volatile matter. These high levels of volatile matter suggest greater ignition efficiency and a higher heating value. The ash content has an inverse relationship with the HHV of a fuel, indicating that a higher ash content results in a lower HHV for the fuel. Additionally, lower ash content suggests a decrease in fouling and slagging during boiler operations. The fixed carbon content was determined to be 15.47 wt% for PN and 17.10 wt% for CNS, which aligns well with the values reported for other biomass feedstocks listed in Table 2. Fixed carbon can be utilised in various applications such as bio-absorbents, soil enhancers, fertilisers, carbon nanotubes, and cosmetic products. Elemental analysis of the two feedstocks demonstrated a higher carbon concentration (PN: 43.90%, CNS: 51.90%) and a lower nitrogen concentration (PN: 0.9%, CNS: 0.7%), suggesting enhanced fuel ignition efficiency and lower NO$_x$ emissions during pyrolysis. The oxygen content was also relatively significant (PN: 48.60%, CNS: 40.10%), consistent with findings from other studies in Table 2. The HHV of CNS (20.86 MJ kg$^{-1}$) was considerably higher than that of PN (15.61 MJ kg$^{-1}$), suggesting that the ignition heat of the fuel would be elevated. Furthermore, the bulk density for PN (391 kg m$^{-3}$) was found to be less than that of CNS (698.70 kg m$^{-3}$), indicating that CNS would be more transportable than PN. The chemical composition of both PN and CNS impacts their

**Table 2** Comparative physicochemical analysis of PN and CNS with other biomass feedstocks

| Parameters | PN | CNS | Groundnut shell[36] | Wood Sawdust[40] |
|---|---|---|---|---|
| **Proximate study (wt%) dry basis** | | | | |
| Moisture content | 3.20 ± 0.10 | 1.50 ± 0.14 | 8.14 ± 0.10 | 3.07 ± 0.10 |
| Volatile content | 79.13 ± 0.40 | 77.10 ± 0.16 | 64.42 ± 0.21 | 80.8 ± 0.30 |
| Ash content | 2.20 ± 0.30 | 4.30 ± 0.12 | 11.73 ± 0.15 | 12.68 ± 0.20 |
| Fixed carbon | 15.47 ± 0.20 | 17.10 ± 0.11 | 15.71 ± 0.10 | 3.38 ± 0.16 |
| | | | | |
| **Elemental analysis (wt%) dry basis** | | | | |
| C | 43.90 ± 0.20 | 51.90 ± 0.15 | 46.89 ± 0.12 | 46.09 ± 0.10 |
| H | 6.60 ± 0.10 | 7.30 ± 0.10 | 7.8 ± 0.16 | 7.02 ± 0.20 |
| N | 0.90 ± 0.20 | 0.70 ± 0.10 | 0.98 ± 0.10 | 0.50 ± 0.20 |
| O | 48.60 ± 0.10 | 40.10 ± 0.20 | 44.23 ± 0.10 | 46.39 ± 0.15 |
| Higher heating value (MJ kg$^{-1}$) | 15.61 ± 0.15 | 20.86 ± 0.10 | 29 ± 0.15 | 18.67 ± 0.10 |
| Bulk density (kg m$^{-3}$) | 391 ± 1.80 | 698.7 ± 1.1 | — | — |
| Hemicellulose | 22.34 ± 0.24 | 51.72 ± 0.31 | — | — |
| Cellulose | 27.62 ± 0.16 | 13.33 ± 0.06 | — | — |
| Lignin | 36.42 ± 0.16 | 21.85 ± 0.12 | — | — |

pyrolytic behavior. PN consists of higher cellulose (27.62 wt%) and lignin (36.42 wt%) but lower hemicellulose (22.34 wt%). The elevated lignin content suggests that PN is likely to yield more biochar, while the cellulose contributes to the generation of bio-oil. On the other hand, CNS has a considerably higher hemicellulose content (51.72 wt%) but lower cellulose (13.33 wt%) and lignin (21.85 wt%) contents. Since hemicellulose decomposes quickly, CNS is anticipated to emit more gases and generate bio-oil with a higher concentration of oxygenated compounds.[39] The characterisation findings for PN and CNS are in good agreement with the biomass data presented in Table 2, affirming that PN and CNS are viable feedstocks for pyrolysis. PN is more suitable for producing biochar and phenolic-rich bio-oil, while CNS is preferred for generating gas and lighter oxygenate yields during pyrolysis.

### 3.2. FTIR of biomass

The functional groups in biomass samples, CNS and PN, were analysed using Fourier Transform Infrared Spectroscopy (FTIR) shown in Fig. 2(a) and (b). The spectra revealed adsorption peaks above 3000 cm$^{-1}$ (CNS: 3001 cm$^{-1}$, PN: 3286 cm$^{-1}$), indicating the presence of water, phenols, acids, and protein impurities due to –OH stretching vibrations.[24] Additionally, peaks observed at 2927 cm$^{-1}$ (CNS), and 2905 cm$^{-1}$ (PN) confirmed the presence of aliphatic hydrocarbons, attributed to C–H stretching of methylene (–CH$_2$–) groups. The characteristic peaks for lignin and protein were identified at 1653 cm$^{-1}$ (CNS) and 1606 cm$^{-1}$ (PN), corresponding to C=C aromatic ring vibrations.[41] Further, peaks around 1400 cm$^{-1}$ (CNS: 1444 cm$^{-1}$, PN: 1406 cm$^{-1}$) indicated the presence of methyl and phenolic groups, attributed to C–H and aliphatic C–H stretching vibrations.[42] The C–O stretching vibration bands observed between 1200–1000 cm$^{-1}$ confirmed the presence of cellulose, corresponding to its glucosic structure; additionally, the feedstocks revealed adsorption bands in the 500–700 cm$^{-1}$ range. Bending vibrations around >700 cm$^{-1}$ corresponded to C–H, while strong C–O stretching vibrations appeared between 1280–1030 cm$^{-1}$.[43]

### 3.3. Thermal profile analysis

The thermal degradation behaviour of hemicellulose, cellulose, and lignin of CNS and PN is shown in Fig. 3(a) and (b). The initial weight loss observed up to 120 °C is due to the evaporation of bound and unbound moisture in the feedstock, resulting in an approximate 5% weight reduction for materials. Hemicellulose decomposition in CNS and PN starts between 180–350 °C, followed by cellulose breakdown in the range of 250–400 °C. The differential thermogravimetry (DTG) curves show a small shoulder peak indicating hemicellulose degradation, while the central peak corresponds to cellulose decomposition. Conversely, lignin degrades over a much wider temperature range (350–900 °C), forming a tailing pattern on the DTG curve. The thermal degradation of CNS and PN biomasses commences with the dehydration phase, characterised by the evaporation of water molecules and light hydrocarbons up to 200 °C, followed by the active pyrolysis stage (200–500 °C), where hemicellulose and cellulose convert into volatile compounds under sustained heating. Lignin decomposition extends over a broader temperature range, contributing to the residual solid fraction. While these temperature ranges are generally consistent for biomass, variations may occur depending on the feedstock composition.[37]

### 3.4. Effect of temperature on product yield

Py-GC/MS analysis of CNS and PN, (Fig. 4(a) and (b)), indicates a temperature-dependent decomposition of biomass into volatile products and residual solids. The pyrolysis behaviour of CNS and PN across temperatures ranging from 400 to 800 °C highlights the effect of thermal degradation on biomass decomposition. At 400 °C, a significant portion of the biomass remains as residue (20.6% ± 1.48% CNS and 26.8% ± 1.34% for
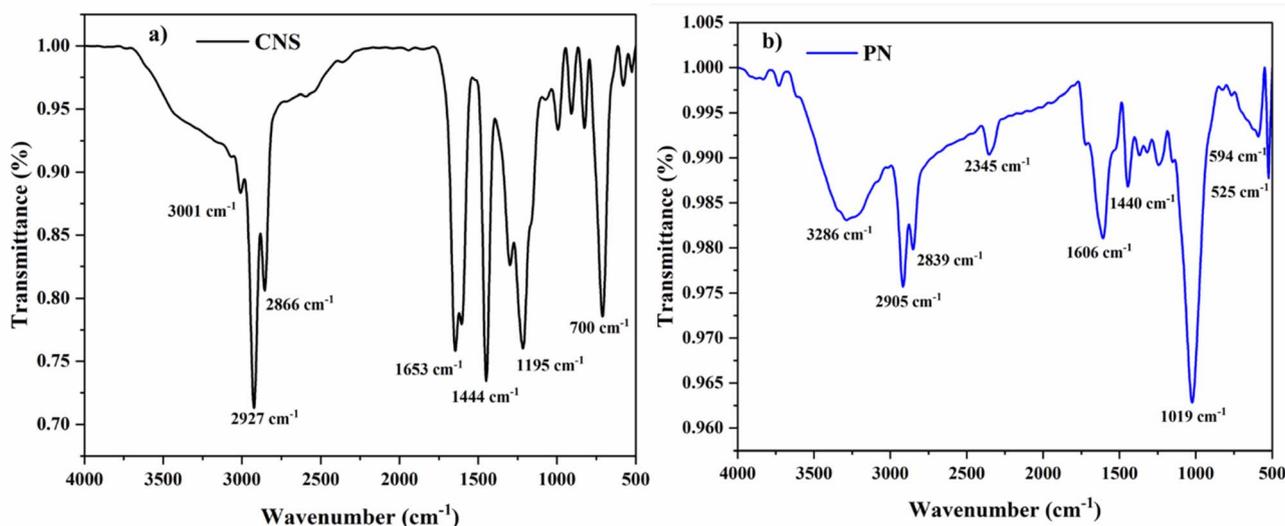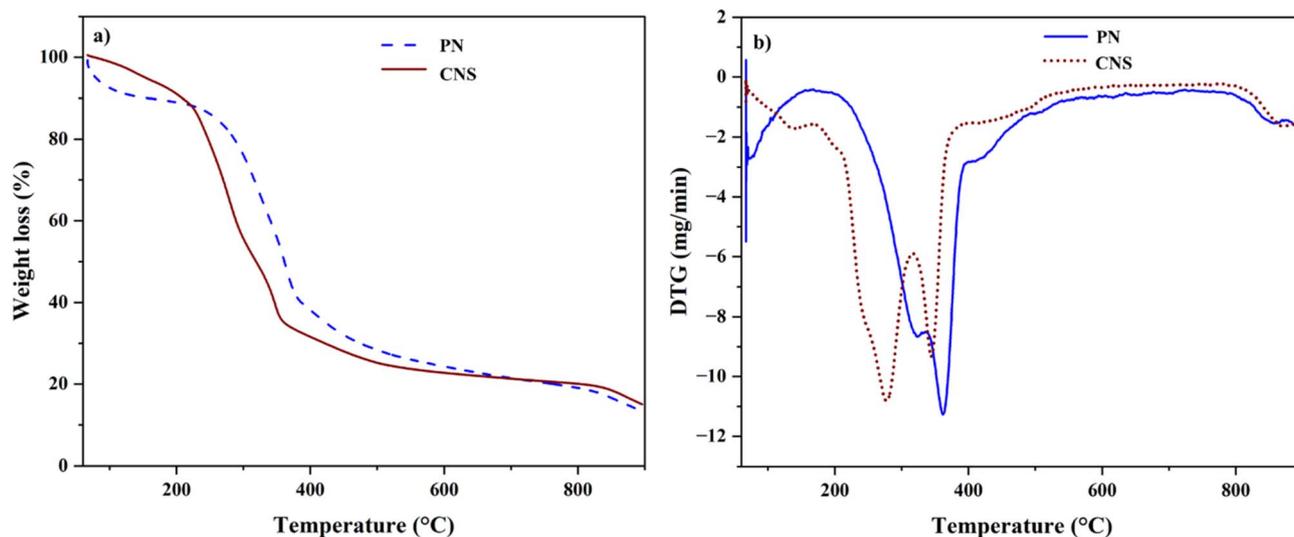


**Fig. 2** FTIR of biomass (a) CNS and (b) PN.

Fig. 3 Thermal degradation analysis: (a) TGA and (b) DTG profiles of pine needle and cashew nut shell biomasses.

PN) due to the incomplete breakdown of lignocellulosic components like lignin, cellulose, and hemicellulose. As the temperature increases to 500 °C, the residue formation decreases to 16.1% ± 0.66% for CNS and 18.5% ± 0.93% for PN. At the same time, the production of volatile compounds increases, reaching 83.9% ± 4.17% for CNS and 81.5% ± 4.07% for PN. This temperature is identified as optimal for bio-oil production.[37–39,44] Beyond 500 °C, the residue levels continue to decline, reaching 2.7% ± 0.14% for CNS and 4.05% ± 0.16% for PN at 800 °C, while volatile yields increase to 97.3% ± 4.87% and 95.95% ± 4.78%, respectively. This is due to secondary cracking reactions that break down heavier compounds into lighter gases, reducing the bio-oil yield. At higher temperatures, lignin undergoes further depolymerisation, enhancing the breakdown of long-chain hydrocarbons and increasing volatile

production. However, excessive temperatures beyond 500 °C can degrade bio-volatile quality by over-cracking valuable intermediates. Thus, maintaining a pyrolysis temperature of 500 °C provides an optimal balance between maximising volatile yields and minimising residue, making it the most favourable condition for bio-oil production. The optimal pyrolysis temperature was determined based on earlier studies of various biomass types, including cotton stalk, groundnut shell, and mustard husk, which were pyrolysed in auger and rotary kiln systems at temperatures ranging from 400 to 700 °C. The findings indicate that the highest oil yield (>45%) is achieved at 500 °C, making this temperature ideal for pyrolysis experiments. As observed in previous studies, the char yield decreases while the gas yield increases with rising temperatures. This study conducted pyrolysis experiments using CNS and PN at an
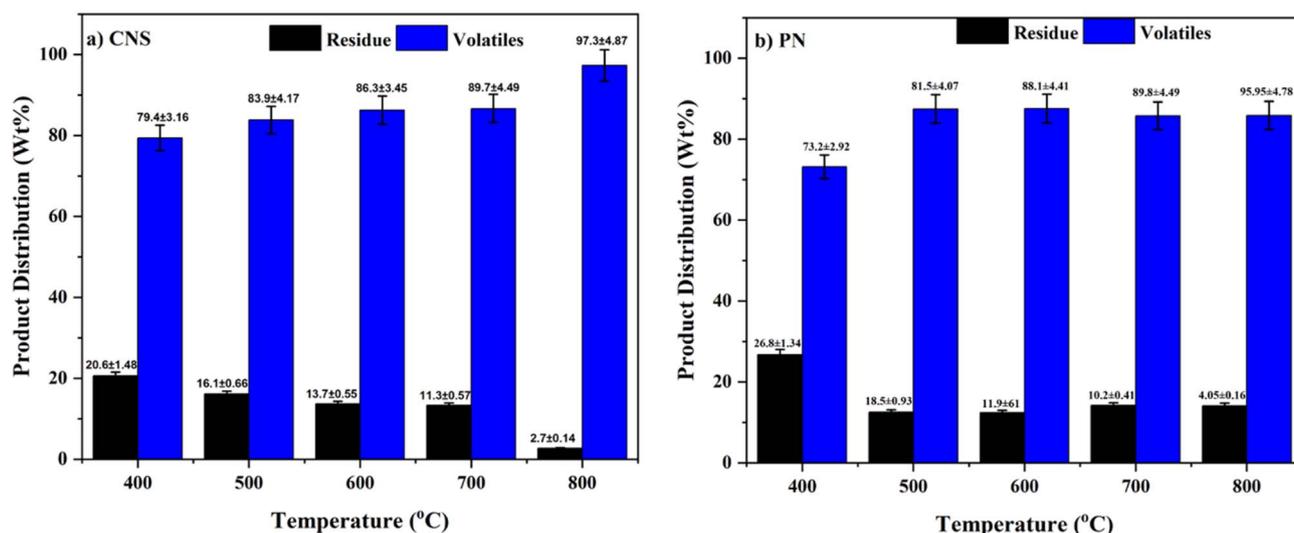


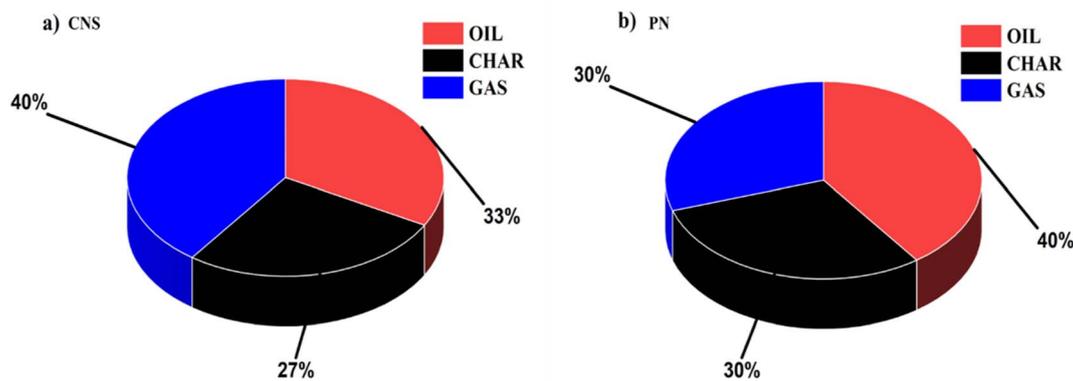Fig. 4 Product yield distribution of (a) CNS and (b) PN at different temperatures in Py–GC/MS system.

**Fig. 5** Product yield distribution of (a) CNS and (b) PN at optimum temperature (500 °C) in rotary kiln reactor system.

optimum temperature of 500 °C in the rotary kiln reactor unit, as shown in Fig. 1(b).

Fig. 5 illustrates the product yield distribution for CNS and PN. Among the two feedstocks, PN (40% ± 5%) produced an oil yield higher than that of CNS (33% ± 5%). Char yield was also observed with PN (30% ± 5%) compared with CNS (27% ± 5%), and gas yield was obtained *vice versa* with CNS (40% ± 5%) and PN (30% ± 5%).[45,46] The higher oil yield from PN can be attributed to its higher volatile matter content and lower lignin levels, which promote oil formation. With its higher lignin content, CNS undergoes increased gasification reactions, producing more significant gas. The differences in product distribution arise from the distinct chemical compositions of these feedstocks. CNS, rich in cellulose and lignin, degrades more slowly, favoring gas formation. Further, PN, with its higher volatile content and lower lignin levels, undergoes faster pyrolysis, leading to higher oil and char yields. This comparison highlights how each feedstock's chemical structure and volatile matter content influence the final distribution of pyrolysis products.

### 3.5. Chemical characterization of pyrolysis product

Py-GC/MS was employed at the laboratory scale to determine the bio-volatile composition of PN and CNS without solvent usage. This method enabled the identification of bio-volatile composition across various temperatures, facilitating the optimization of pyrolysis conditions. By analysing the impact of feedstock type and temperature, Py-GC/MS revealed distinct bio-volatile compositions, with PN and CNS containing phenolic-rich volatiles at 500 °C. This approach provided critical data on the temperature at which targeted compounds were maximized, for further performing scale-up experiments. The solvent-free analysis ensured precise insights into the chemical composition, establishing a strong basis for scalable bioenergy production. These findings were essential for transitioning from laboratory insights to practical, sustainable applications.

The rotary kiln reactor was utilized in pilot-scale studies to produce bio-oil from PN and CNS at an optimized temperature of 500 °C, evaluating yield and phenolic concentration. Unlike Py-GC/MS, bio-oil composition was analysed using solvent extraction followed by gas chromatography-mass spectrometry (GC/MS), ensuring accurate characterization. This setup validated the scalability of the pyrolysis process while maintaining product consistency and efficiency. The resulting bio-oil, also enriched with phenolics and aromatics. The rotary kiln experiments demonstrated a practical pathway for transforming underutilized biomass into high-value products. This dual-scale approach is vital in advancing the circular bioeconomy by reducing reliance on fossil fuels. The differences between the rotary kiln and Py-GC/MS products arise mainly from variations in heating rate, vapor residence time, secondary reactions, and operational scale. Py-GC/MS involves extremely high heating rates and very short residence times, favouring the release of primary volatiles with minimal secondary transformations. In contrast, the rotary kiln operates at slower heating rates and longer vapor residence times, which promote secondary cracking, deoxygenation, and char–vapor interactions, altering product composition. Scale effects further contribute, as the rotary kiln introduces temperature gradients and heterogeneous heating, unlike the controlled conditions of Py-GC/MS, thereby leading to distinct product distributions.

**3.5.1. Compositional of pyrolysis volatiles.** Fig. 6(a) illustrates the temperature-dependent distribution of chemical families in bio-volatiles from pyrolysis of PN biomass at temperatures ranging from 400 to 800 °C. At lower temperatures (400–500 °C), oxygenated compounds are predominant, making the bio-volatiles suitable for chemical feedstocks. Acids remain stable up to 700 °C but increase at 800 °C due to the decomposition of lignocellulose, with *n*-hexadecenoic acid, *cis*-10-heptadecenoic acid, dodecanoic acid, and oleic acid being the major constituents. Aldehydes are present at intermediate temperatures (500–600 °C) but disappear at 800 °C, with 2-propenal being the predominant type. Ketones are most abundant at 400 °C, with key compounds including cyclopentanone, 2-methyl-2-cyclopenten-1-one, ethenone (1-(2-furanyl)-), and acetophenone. Furans decompose as the temperature increases, including tetrahydrofurfuryl chloride and benzofuran (4,7-dimethyl-). Phenolics peak at 600 °C, decline at 700 °C, and rise again at 800 °C, with primary components being 2-methoxyphenol, *p*-cresol, and 4-ethyl-2-methoxyphenol.[47]
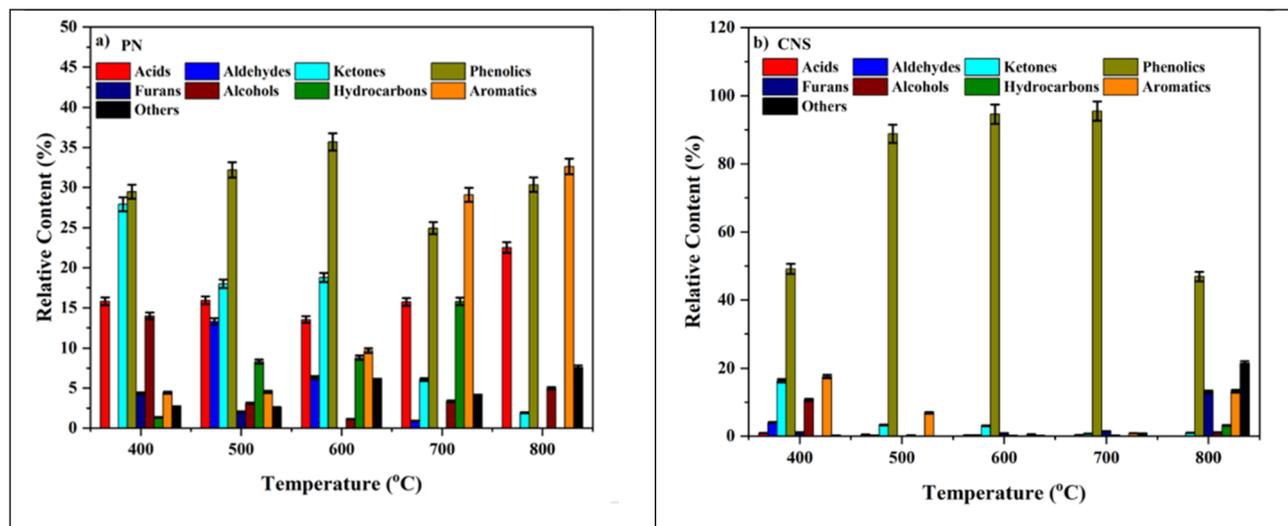
Fig. 6 Comparison of chemical composition of bio-volatiles at different temperatures from (a) PN and (b) CNS.

Varma and Mondal (2018) observed similar trends in their pyrolysis studies of PN at around 550 °C.[25] Alcohols generally decrease with temperature but show a slight increase at 800 °C. Hydrocarbons peak at 700 °C, with dodecane, pentadecane, tetradecane, and 2-methyl hexacosane as dominant species, but disappear at 800 °C. Due to condensation reactions, the production of aromatic compounds significantly increases at higher temperatures, with mesitylene, naphthalene, and *o*-xylene as key constituents. A nitrogen-containing fraction increases at higher temperatures. Overall, lower temperatures favour the formation of oxygenated compounds, making the bio-volatiles valuable for chemical applications. Higher temperatures (700–800 °C) enhance aromatic production, making them more suitable for energy and fuel applications.[48]

Fig. 6(b) illustrates the variations in bio-volatiles from CNS pyrolysis as they depend on temperature. At lower temperatures, acids, aldehydes, and alcohols are the primary compounds detected; however, their levels decline as temperature increases, indicating that they decompose into less significant volatile compounds. Furthermore, the concentration of phenolics significantly increases, reaching 95.53%, which highlights their thermal stability and lignin-derived origin. Kaur *et al.* (2013) observed a similar trend in slow pyrolysis (300–500 °C), with phenolics as dominant compounds.[49] Major phenolic components include (*Z*)-3-(pentadec-8-en-1-yl)phenol, 2-methoxyphenol, creosol, and 2,6-dimethoxyphenol; these findings are supported by research conducted by Ratima Wai-tongkham *et al.* (2023) using microwave pyrolysis. Ketones and furans generally decrease with increasing temperature, although furans tend to increase slightly at higher temperatures, likely due to carbohydrate breakdown.[48] Identified ketones include 1,2-cyclopentadiene and 2-methyl-2-cyclopenten-1-one, while benzofuran is the primary furan derivative. Aromatic compounds decline at higher temperatures, possibly converting into phenolics, with key components including 1,2,3-trimethoxy-5-methylbenzene and naphthalene.

Hydrocarbons only appear at the highest temperature, indicating molecular breakdown, with oxirane and tetradecane as primary representatives. Additionally, the production of small molecules and gases increases, reflecting extensive thermal degradation. These findings emphasise the impact of pyrolysis conditions on bio-oil composition, which is necessary for energy applications. Das *et al.* reported similar trends in fixed-bed pyrolysis of cashewnut biomass.[50]

A comparative analysis of the Py-GC/MS profiles of PN and CNS biomass highlights temperature-driven variations in chemical composition, with distinct differences in the distribution of chemical families. In PN biomass, thermal decomposition at lower temperatures (400–500 °C) primarily produces oxygenated compounds such as acids, aldehydes, and phenolics. As the temperature rises (700–800 °C), a noticeable shift toward forming aromatics and hydrocarbons enhances its suitability for energy applications. The concentrations of ketones and furans decrease significantly with increasing temperature, while the alcohol level rises slightly at 800 °C. Furthermore, CNS biomass exhibits a substantial increase in phenolics at higher temperatures, reaching up to 95.53%, which indicates thermal stability. At the same time, the amounts of acids, aldehydes, and alcohols decrease. Ketones and furans also decrease, except for a slight increase at higher temperatures, likely due to the breakdown of carbohydrates. Hydrocarbons appear only at the highest temperature.[51] Suggesting that larger molecules break down through thermal cracking. These results show that both feedstocks have fewer oxygenated compounds and more aromatics as the temperature increases. However, CNS biomass retains its phenolics more effectively, which is a promising option for bio-refining. At the same time, PN biomass produces more aromatic hydrocarbons, which makes it better suited for fuel upgrading.

**3.5.2. Elemental composition of pyrolysis oil.** Table 3 presents the elemental composition, atomic ratios, HHV, and pH of the char and oil produced from CNS and PN by pyrolysis.

**Table 3**  Physicochemical characterzation of PN and CNS of pyrolysis oil and biochar

| Feed | Product | Nitrogen (N)% | Carbon (C)% | Hydrogen (H)% | Oxygen (O)% | H/C | O/C | HHV (MJ Kg$^{-1}$) | pH |
|------|---------|---------------|-------------|---------------|-------------|-----|-----|---------------------|-----|
| CNS | Char | $1.98 \pm 0.05$ | $80.42 \pm 2.41$ | $4.01 \pm 0.16$ | $13.59 \pm 0.54$ | $0.6 \pm 0.018$ | $0.13 \pm 0.003$ | $30.54 \pm 0.91$ | $8.9 \pm 0.2$ |
|  | Oil | $1.71 \pm 0.04$ | $55.91 \pm 2.23$ | $10.39 \pm 0.41$ | $31.99 \pm 1.59$ | $2.23 \pm 0.08$ | $0.43 \pm 0.017$ | $28.14 \pm 1.12$ | $4.4 \pm 0.13$ |
| PN | Char | $1.68 \pm 0.06$ | $78.16 \pm 2.34$ | $3.31 \pm 0.13$ | $16.85 \pm 0.67$ | $0.51 \pm 0.01$ | $0.16 \pm 0.008$ | $28.18 \pm 1.40$ | $9.4 \pm 0.37$ |
|  | Oil | $1.53 \pm 0.03$ | $67.16 \pm 2.68$ | $11.09 \pm 0.44$ | $20.22 \pm 1.01$ | $1.98 \pm 0.09$ | $0.23 \pm 0.011$ | $35.08 \pm 1.40$ | $3.8 \pm 0.11$ |

There are clear differences in product quality. CNS char has a slightly higher carbon content (80.42%) and hydrogen content (4.01%) than PN char, which has 78.16% carbon and 3.31% hydrogen. This means CNS char has a higher HHV of 30.54 MJ kg$^{-1}$ compared to 28.18 MJ kg$^{-1}$ for PN char, making CNS char a better solid fuel whereas PN oil has better fuel properties. It contains more carbon (67.16%) and hydrogen (11.09%) than CNS oil, which has 55.91% carbon and 10.39% hydrogen. PN oil also has a lower oxygen content at 20.22% compared to CNS oil's 31.99%. This lower oxygen content improves fuel quality and increases the heating value. However, bio-oil usually contains more oxygen than regular petroleum fuels. This high oxygen content indicates the presence of highly polar compounds, which contribute to its high viscosity and boiling point.[52] The HHV of PN oil is significantly greater at (35.08 MJ kg$^{-1}$).[53] Compared to CNS oil, which has an HHV of (28.14 MJ kg$^{-1}$). Fig. 7 (Van Krevelen diagram (H/C *vs.* O/C)) provides a clear representation of the elemental characteristics of the oils and chars produced from PN and CNS. CNS-derived oil exhibits a higher H/C ratio and slightly elevated O/C ratio compared to PN oil, indicating a relatively hydrogen-rich but more oxygenated product. The PN oil occupies a region that corresponds to moderate deoxygenation with a balanced hydrogen content. The chars generated from both feedstocks appear in the low H/C and low O/C region, indicating significant aromatic condensation and carbon enrichment during pyrolysis. Overall, the diagram effectively highlights the differences in deoxygenation patterns between the two biomass, supporting the comparative evaluation of their fuel-quality characteristics. Eqn (6) and (7)

represent the H/C and O/C ratios calculations regarding pH, CNS char has a slightly alkaline pH of 8.9, while CNS oil is acidic with a pH of 4.3. Similarly, PN char is more alkaline, with a pH of 9.4, whereas PN oil is highly acidic, with a pH of 3.8. The alkaline nature of the chars indicates their potential suitability for applications such as soil amendment or adsorbents. At the same time, the acidic nature of the oils suggests the presence of organic acids and other acidic compounds, which may require upgrading during fuel treatment. CNS is more effective in producing high-energy char, while PN excels in generating high-quality pyrolysis oil. This highlights the importance of feed-stock properties in determining product yields and applications.

**3.5.3.  GC/MS analysis.** Fig. 8(a) illustrates the chemical composition distribution from the pyrolysis of PN biomass at an optimised temperature of 500 °C from both the reactor systems, (Tables TS1 and TS2). The bio-oil exhibited a high yield of hydrocarbons (45%) and phenolics (23.82%).[54] Highlighting the significant role of lignin decomposition. Aromatic hydrocarbons were primarily generated through secondary reactions.[55] Such as the cracking and polymerization of volatile intermediates. The primary aromatic hydrocarbons identified included 1-pentadecene, 1-decene, toluene, 1-undecene, and *o*-xylene. The phenolics were derived directly from lignin depolymerization, as confirmed by Thangalazhy *et al.*, noted that phenols are produced from lignin[54–56] The observed phenolic compounds included 2-methoxyphenol, *p*-cresol, 2-methylphenol, 4-ethyl-2-methoxyphenol, and 2-methoxy-5-methylphenol. The degradation of hemicellulose and cellulose also contributed to a relatively high content of acids (13.31%), with key components such as *n*-hexadecenoic acid, *cis*-10-heptadecenoic acid, dodecanoic acid, and oleic acid. Sharma *et al.* also reported a similar acid content of 15% in pine needle bio-oil, aligning with other chemical compositions observed.[57] Additionally, the thermal breakdown of polysaccharides produced ketones (5.29%) and furans (1.2%). Major ketones included 2-cyclopenten-1-one, 2,3-dimethyl-, cyclopentanone, and ethanone, 1-(2-furanyl)-. Furthermore, tetrahydrofurfuryl chloride, benzofuran, and 4,7-dimethyl were observed as furans. The bio-oil also contained aliphatic hydrocarbons (6.28%), such as 2-methyl hexaoxane, dodecane, pentadecane, tetradecane, and undecane, which partially deoxygenated the bio-oil, improving its fuel quality. Furthermore, the analysis detected smaller fractions of alcohol (2.9%), aldehydes (1.2%), and trace compounds (4.45%), emphasizing the complex nature of the bio-oil derived from PN. These compounds are likely formed due to the thermal degradation of cellulose and hemicellulose. Overall, the composition
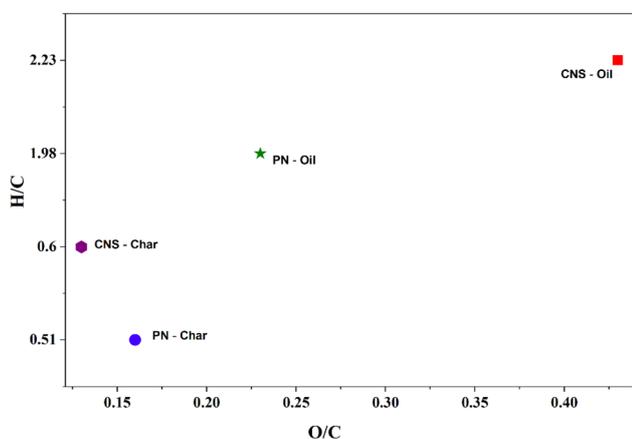


**Fig. 7**  H/C *vs.* O/C (van Krevelen) plot for bio-oil and char derived from PN and CNS.
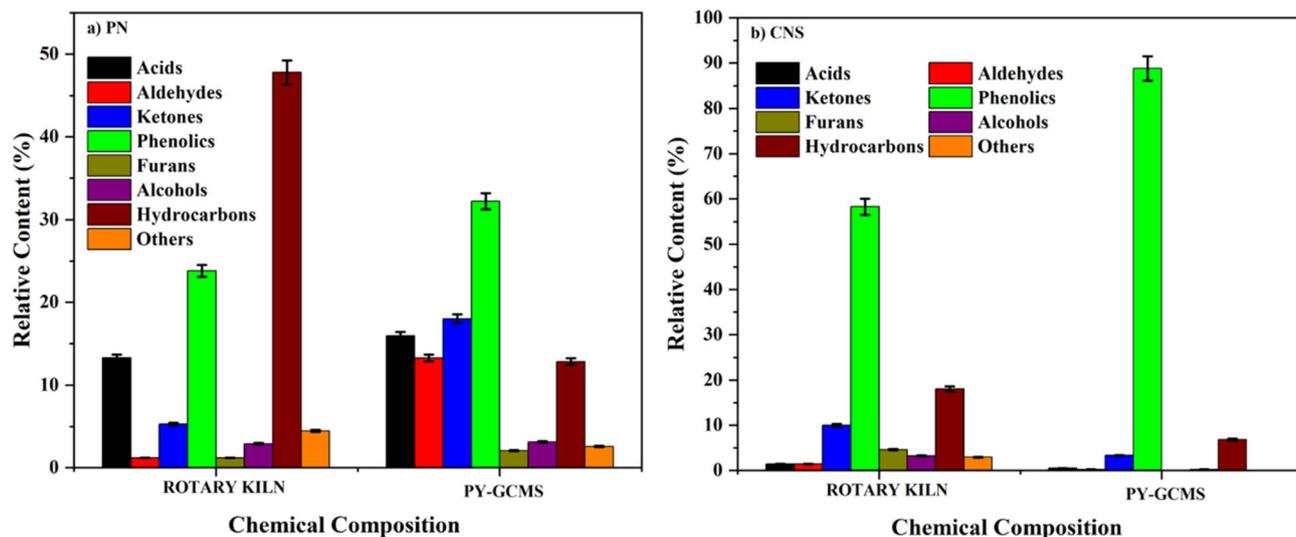
Fig. 8 Chemical composition of oil at optimum temperature (500 °C) from different reactor systems with different feedstocks (a) PN and (b) CNS.

of the bio-oil is consistent with the findings reported in the literature.[57]

Fig. 8(b) illustrates that at an optimized pyrolysis temperature of 500 °C, CNS biomass produced oil with a high concentration of phenolics (58.27%) and hydrocarbons (15.19%), which highlights the lignin-rich nature of the feedstock. The significant phenolics identified included (*Z*)-3-(pentadec-8-en-1-yl)phenol, 2-methoxyphenol, creosol, 4-ethyl-2-methoxyphenol, *p*-cresol, 2,6-dimethoxyphenol, and 2-methylphenol. Significant aromatic hydrocarbons formed through secondary reactions of volatiles included benzene, 1,2,3-trimethoxy-5-methylbenzene, 3,5-dimethoxy-4-hydroxytoluene, 2-methyl-2-cyclopenten-1-one, and 1-methyl-naphthalene. The decomposition of cellulose and hemicellulose prominently produced ketones (10.02%) and furans (4.6%). Key ketones observed were 1,2-cyclopentanedione (3-methyl-), 2-cyclopenten-1-one (3-methyl-), and cyclopentanone. At the same time, furans included isoavocadienofuran, (*E*)-2-(pentadeca-1,14-dien-1-yl) furan, and 2-furanmethanol. Low concentrations of acids (1.44%) and aldehydes (1.43%) indicated effective thermal cracking, which reduced oxygenated compounds and enhanced oil stability. The significant acids identified were *n*-hexadecenoic acid, 2-tricosanoic acid, pentatonic acid, and 3-methyl-. Moderate levels of alcohol (3.24%) and aliphatic hydrocarbons (2.87%) further improved the fuel properties of the oil. The carbon distribution range for the volatile chemical compounds in the bio-oil spans from C5 to C30, making it comparable to other petroleum fuels.[58]

A comparative analysis of the oil composition from PN and CNS biomass at an optimised pyrolysis temperature of 500 °C highlights the influence of feedstock properties on the chemical distribution. The oil derived from PN exhibited a significantly higher concentration of aromatics (41.52%) than CNS oil (15.19%), indicating extensive secondary reactions and cracking of volatiles in PN. Comparatively, CNS oil was dominated by

phenolic compounds (58.27%), reflecting the lignin-rich nature of the feedstock.[59] While PN oil contained a lower phenolic content (23.82%). The higher concentration of phenolic compounds in CNS oil presents significant challenges for using pyrolysis bio-oil as fuel, primarily due to the increased viscosity associated with these compounds.[60,61] PN produced higher acids (13.31%) and hydrocarbons (6.28%), primarily due to the degradation of hemicellulose and cellulose.[62] CNS oil showed lower acid content (1.44%) and hydrocarbon content (2.87%), suggesting more effective deoxygenation. CNS oil also contained higher levels of ketones (10.02%) and furans (4.6%), which originated from the breakdown of cellulose and hemicellulose.[63] PN produced lower amounts of these compounds, with only 5.29% ketones and 1.2% furans. The feedstock showed minor contributions from alcohol and aldehydes, with slightly higher concentrations in CNS oil. From Fig. 8(a) and (b), it is observed that the chemical composition (Tables TS1 and TS2) of bio-oil/volatiles from PN and CNS varies significantly between the two reactor systems, namely the rotary kiln and Py-GC/MS. This is due to differences in feedstock composition and pyrolysis conditions (slow and fast pyrolysis). PN bio-oil shows higher hydrocarbon content in the rotary kiln due to enhanced deoxygenation and thermal cracking, while CNS is dominated by phenolics, reflecting its high lignin content. In Py-GC/MS, both feedstocks were observed with increased phenolic content due to rapid lignin decomposition under fast pyrolysis conditions. In the case of PN, higher acids and ketones were observed due to the decomposition of hemicellulose and cellulose, whereas CNS, with a lower hemicellulose content, generates fewer aldehydes and furans, favouring direct lignin-to-phenolics conversion. Based on the above discussion, it is observed that reactor conditions and feedstock composition play a crucial role in determining the chemical composition of bio-oil, which in turn affects its suitability for use as a fuel or in chemical applications.

Fig. 9 illustrates the systematic conversion of lignocellulosic biomass, such as PN and CNS, into valuable bio-based chemicals through pyrolysis and subsequent transformation pathways. Initially, the biomass, which contains cellulose, hemicellulose, and lignin as its three primary structural polymers, undergoes thermal decomposition under limited oxygen conditions during pyrolysis, resulting in the evolution of bio-volatiles along with biochar and non-condensable gases. These bio-volatiles serve as precursors for multiple classes of organic compounds.[55] The cellulose fraction, a polysaccharide composed of β-1,4-linked glucose units, thermally decomposes to form smaller oxygenated intermediates, such as levoglucosan and hydroxyacetaldehyde, which subsequently transform into furan and its derivatives through dehydration and rearrangement reactions.[57] Simultaneously, the hemicellulose component, being more amorphous and thermally labile, decomposes at lower temperatures to yield light oxygenates, including acetic acid, furfural, and pyran-type compounds that further undergo cyclisation and nitrogen incorporation reactions to form pyridines and their derivatives.[58] The lignin exhibits a broader thermal decomposition range, generating a variety of phenolic compounds, including phenol, cresol, catechol, guaiacol, and syringol, through the cleavage of ether and carbon–carbon linkages within its macromolecular structure. These three decomposition routes collectively contribute to the pool of bio-volatiles, which contain furans, pyridines, and phenolic derivatives, crucial intermediates for renewable fuels and speciality chemicals.[59] As the pyrolysis temperature
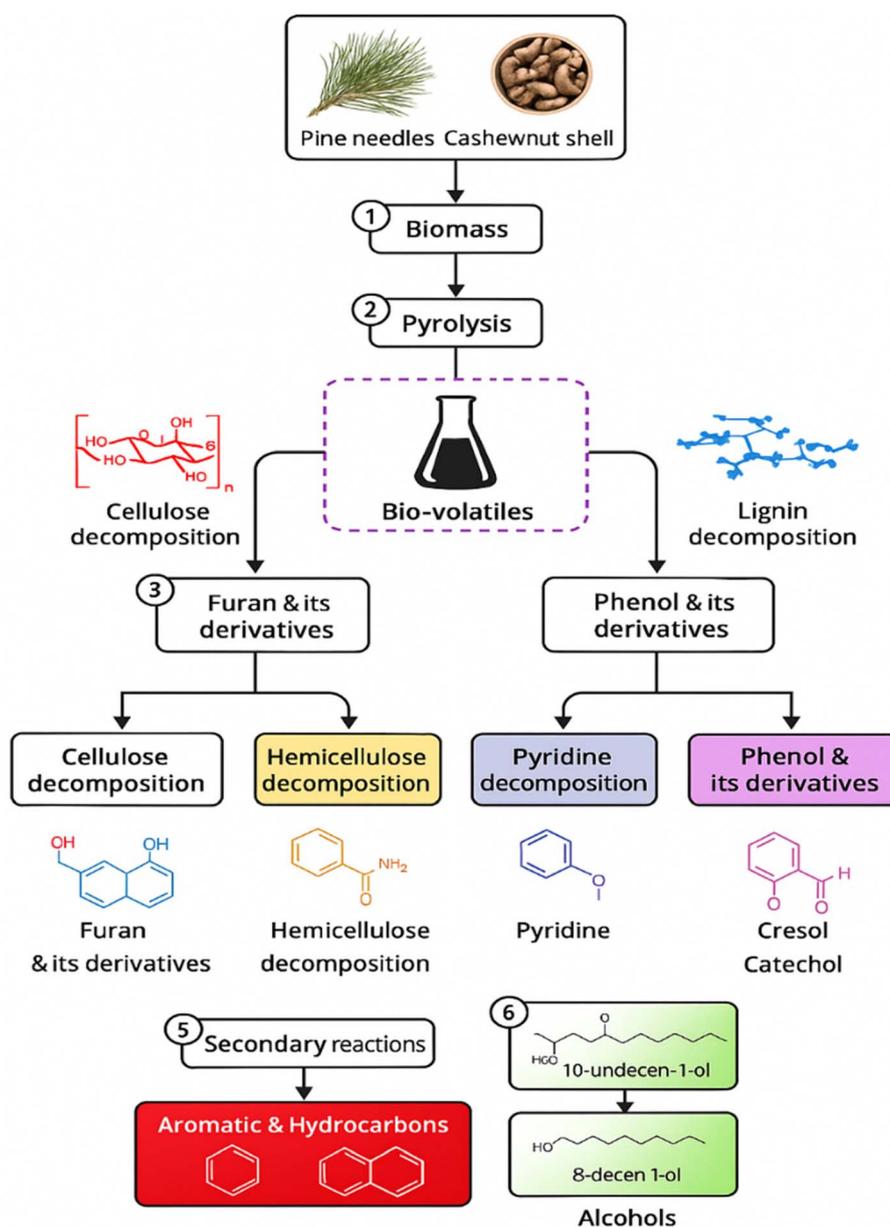


Fig. 9 The systematic conversion of lignocellulosic biomass into valuable bio-based chemicals.

increases, secondary reactions, including condensation, deoxygenation, cracking, and aromatisation, occur, converting unstable oxygenates into more stable aromatic and hydrocarbon compounds, such as benzene, toluene, and naphthalene. This process enhances the energy density and stability of bio-oil. In parallel, partial reduction of oxygenated intermediates leads to the formation of long-chain alcohols such as 10-undecen-1-ol and 8-dodecen-1-ol, which are of industrial importance as fragrance precursors, solvents, and intermediates for bio-lubricants.[60] The logic of this transformation process is grounded in the distinct chemical nature and thermal behavior of the biomass constituents: cellulose primarily yields carbohydrate-derived oxygenates and furans due to its linear polymeric nature; hemicellulose contributes nitrogenous and oxygen-rich heterocycles like pyridines because of its mixed sugar and acetylated structure; while lignin, being inherently aromatic, serves as the primary source of phenolic and aromatic hydrocarbons.[61] The stepwise degradation pathway thus integrates chemical selectivity with thermochemical dynamics, enabling the valorization of low-cost agricultural and forest residues into a wide spectrum of high-value compounds. Overall, this process represents an efficient and sustainable route for biomass valorization, promoting circular bioeconomy principles by transforming renewable waste materials into functional chemicals and potential biofuels through controlled pyrolysis and subsequent chemical transformations.

**3.5.4.   FESEM analysis of biochar.** The surface morphology of the biochar, analyzed using scanning electron microscopy (SEM), is shown in Fig. 10. It reveals that the biochar samples develop pores due to the removal of volatile components during pyrolysis. Morphological differences between PN and CNS biochar's are evident: PN biochar exhibits a more layered and porous texture, while CNS biochar shows elongated, irregular pore structures. Literature indicates that biochar, including that derived from PN, can act as an effective support material when combined with metal-modified catalysts. Such combinations in catalytic pyrolysis have been observed to facilitate deoxygenation, reduce the fraction of oxygenated compounds,

and enhance the production of hydrocarbons and aromatics.[62] Furthermore, the inherent mineral content in biomass-derived chars may also contribute to catalytic activity during thermochemical conversion, influencing product yield and quality. In addition to such catalytic potential, the observed pore structures in both PN and CNS biochar's suggest suitability for adsorption, soil amendment, and water treatment applications.[63] Overall, SEM morphology highlights the structural diversity of PN *vs.* CNS biochar's and underscores their broad potential in environmental and energy-related uses. The surface morphology of the biochar, analyzed using SEM, (Fig. 10). The observed pore formation can primarily be attributed to the loss of volatile matter from the biochar surface during pyrolysis. The SEM images reveal apparent differences in the surface structures of biochar derived from PN and CNS. PN biochar exhibits a layered structure with visible pores, while CNS biochar displays long, irregularly shaped pores. These pore formations observed in SEM images suggest potential structural characteristics that may support various applications. Studies have shown that porous structures in biochar, as observed in SEM, contribute to its suitability for applications such as improving soil quality, adsorption, and water filtration. Overall, these SEM images highlight the strong potential of both biochars for environmental applications.

### 3.6.   Plausible mechanism

Fig. 11 illustrates the mechanism behind the two different feedstocks, namely PN and CNS, which pyrolyze similarly but produce distinct products due to differences in their lignocellulosic composition. The pyrolytic conversion of PN and CNS into bio-volatile compounds is further classified into various chemical groups. The process begins with biomass pyrolysis, where the lignocellulosic components (cellulose, hemicellulose, and lignin) break down into different bio-based compounds. The primary products include furan and its derivatives derived from hemicellulose degradation. Pyridine derivatives originate from nitrogen-containing biomass fractions. Phenols and their derivatives result from lignin decomposition, leading to further transformation into aromatic hydrocarbons. Additionally,
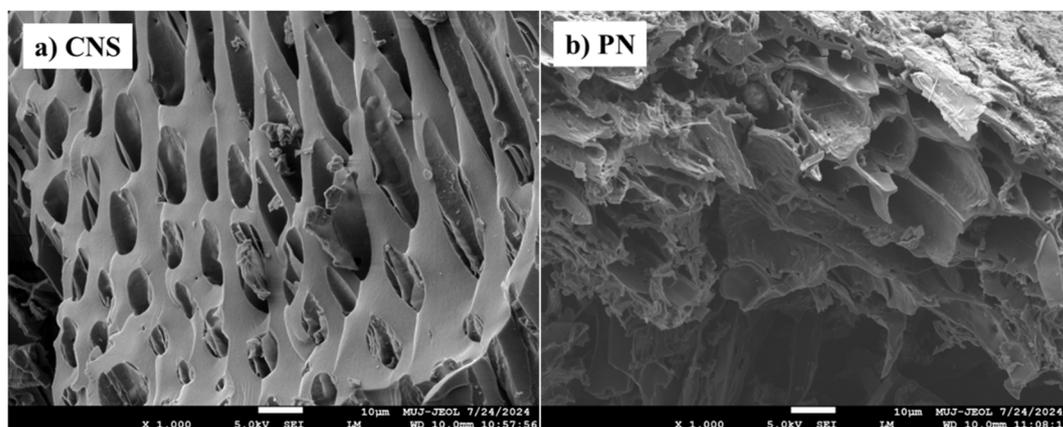
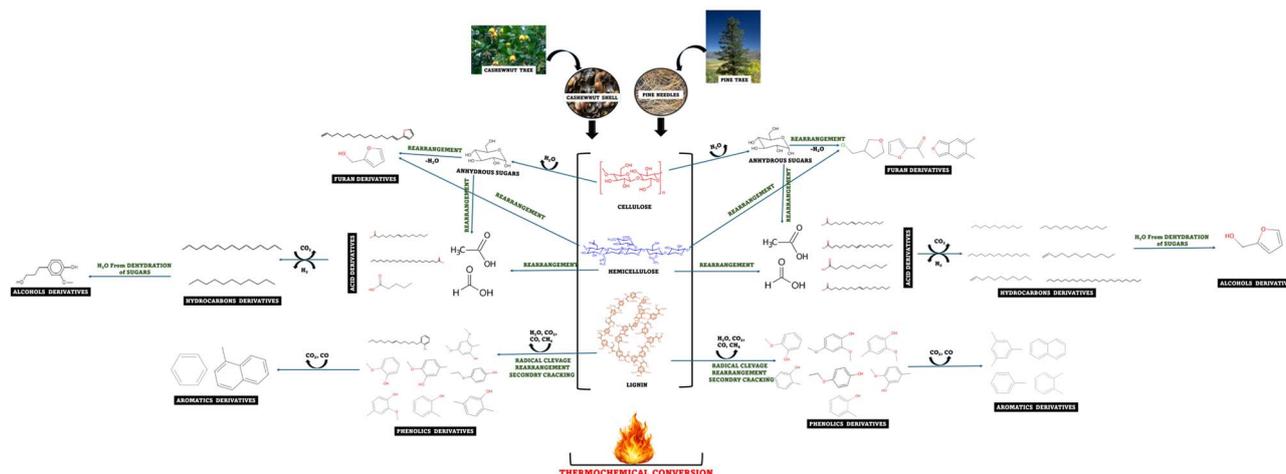Fig. 10   SEM images of (a) CNS and (b) PN.

**Fig. 11** Mechanism of pyrolysis of PN and CNS for bio-oil production and chemical composition.

alcohols, like 8-dodecen-1-ol and 10-undecen-1-ol, are produced, possibly from lipid fractions or secondary reactions. This pathway highlights the potential of biomass pyrolysis to generate high-value biochemicals, which can be utilised in fuel, pharmaceutical, and polymer industries. PN generate phenolic chemicals, aromatic hydrocarbons, and light oxygenates due to their high lignin and hemicellulose content. PN have a high concentration of lignin, which leads to significant bond breakage during pyrolysis. The breakdown of hemicellulose in PN also contributes to the production of light oxygenates, such as ketones and aldehydes, which further influence the composition of the bio-oil. However, with higher cellulose and moderate lignin levels, CNS produce sugars, alcohol, and lighter hydrocarbons. The depolymerisation of cellulose leads to the formation of anhydrous sugars, such as levoglucosan, which can dehydrate furans and other oxygenated hydrocarbons. Although the hemicellulose content in CNS is lower than in PN, it still produces some light oxygenates. The lignin found in CNS produces fewer phenolic compounds but results in a distinct profile of alkylated aromatics, influenced by the unique structural characteristics of the lignin and the presence of extractives in the feedstock. Secondary cracking reactions occur more frequently in CNS, leading to a higher yield of lighter hydrocarbons and oxygenates. The compositional differences between these feedstocks have a significant impact on the pyrolysis process and the properties of the resulting bio-oil. PN are more suitable for producing aromatic-rich bio-oil, while cashew nut shells provide a balanced product profile with significant quantities of sugars, alcohol, and lighter hydrocarbons. These findings highlight the essential importance of feedstock selection in optimising pyrolysis processes to achieve desired bio-oil compositions. The differences in the lignocellulosic structures of PN and CNS not only influence the pyrolysis pathways but also determine the physicochemical properties of the resultant bio-oils. PN, with higher lignin content, yield phenolic-rich fractions and aromatic hydrocarbons that impart higher thermal stability and energy density but also increase viscosity. The oxygenates from hemicellulose breakdown

contribute to acidity and reduced stability. Conversely, CNS, dominated by cellulose, produce levoglucosan, furans, and light alcohols, leading to bio-oils with relatively higher oxygen content and lower heating value but improved miscibility with polar solvents. The lower lignin-derived phenolics in CNS oil reduce viscosity, whereas the higher fraction of alkylated aromatics enhances volatility. Thus, the structural features of each feedstock directly translate into the functional properties of the bio-oil, underscoring the importance of the structure property relationship in biomass selection for pyrolysis applications.

## 4. Limitations and future research directions

Despite the promising results, this study has several limitations that must be addressed to enhance the efficiency and commercial feasibility of biomass pyrolysis. Bio-oil high oxygen content and poor stability lead to high viscosity, corrosiveness, and a low calorific value, complicating its use as a fuel and necessitating advanced separation techniques, such as liquid–liquid extraction. Feedstock variability, such as differences in PN and CNS due to geographic location, harvest season, or storage, affects pyrolysis behaviour and product consistency. Scaling our semi-pilot rotary kiln reactor to industrial levels presents engineering and economic challenges, including achieving uniform heat transfer, maintaining continuous operation, and optimising energy efficiency. High energy input at elevated temperatures may offset environmental benefits. By-product management, including biochar disposal and non-condensable gas emissions, requires evaluation for sustainability. Future research should prioritise improving bio-oil quality through liquid–liquid extraction to separate oxygenates and enhance fuel properties. Feedstock pre-treatment methods (such as torrefaction, solvent extraction, and biological methods) can enhance thermal degradation and improve bio-oil yield. In our study, we utilised a rotary kiln reactor and

the process was operated at a fixed heating rate to isolate the effect of temperature. Accordingly, future studies should systematically investigate the combined influence of heating rate, residence time, and temperature on pyrolysis product selectivity and bio-oil quality, thereby enabling a more comprehensive understanding of the interactions between these process parameters. Still, future work could explore alternative designs, such as fluidised bed, microwave-assisted, or plasma pyrolysis, to enhance heat transfer and product selectivity. Computational modelling and process simulation can optimise reactor performance. Integrating pyrolysis with a circular economy by utilizing syngas for power generation or extracting high-value chemicals from bio-oil *via* separation techniques can improve economic viability. Further exploration of biochar applications in soil remediation, carbon sequestration, and wastewater treatment, including functionalization for heavy metal (HMs) adsorption, will enhance the sustainability of these processes. These advancements will support large-scale biofuel production and waste valorisation, thereby reducing dependence on fossil fuels.

## 5. Conclusions

This study systematically investigated the pyrolysis of PN and CNS to produce renewable bio-oils and value-added products using a dual-scale approach. This approach integrated analytical Py-GC/MS studies with a semi-pilot rotary kiln reactor. The impact of pyrolysis temperature (400 °C to 800 °C) on product yields and chemical composition was extensively assessed. The findings indicated that 500 °C maximises bio-oil production while maintaining a favourable chemical profile. PN yielded a higher bio-oil fraction (40%), primarily composed of aromatic compounds, making it highly suitable for use as a fuel. Cashew nut shells produced a phenolic-rich bio-oil (33%), demonstrating potential for use in the chemical industry. Gas yields depended on the feedstock, with CNS generating 40% gas and PN yielding 30%, reflecting their intrinsic compositional differences. Elemental analysis confirmed that PN-derived bio-oil had superior higher heating values (35.08 MJ kg$^{-1}$) compared to CNS (28.14 MJ kg$^{-1}$), highlighting its potential for energy applications. Biochar obtained from both feedstocks was also subjected to FESEM analysis to observe its surface properties. These findings demonstrate that optimised pyrolysis conditions and feedstock-specific behaviours can effectively tailor bio-oil composition and enhance the valorisation of underutilised biomass residues into renewable fuels and value-added chemicals.

## Conflicts of interest

The authors declare that they have no known competing financial interests or personal relationships that could have appeared to influence the work reported in this paper.

## Data availability

The data will be available on request.

Supplementary information (SI): detailed Py-GC/MS chemical composition data of bio-oil derived from pine needles and cashew nut shells at 500 °C, including identified compounds, molecular formulas, retention times, and relative area percentages (Tables TS1–TS2). See DOI: https://doi.org/10.1039/d5ra08244g.

## References

1 S. Dey, A. Sreenivasulu, G. T. N. Veerendra, K. V. Rao and P. S. S. A. Babu, *Innov. Green Dev.*, 2022, **1**, 100006.

2 Y. A. Begum, S. Kumari, S. K. Jain and M. C. Garg, *Environ. Sci.:Adv.*, 2024, **3**, 1197–1216.

3 K. K. Jaiswal, C. R. Chowdhury, D. Yadav, R. Verma, S. Dutta, K. S. Jaiswal, B. Sangmesh and K. S. K. Karuppasamy, *Energy Nexus*, 2022, **7**, 100118.

4 H. M. Saleh and A. I. Hassan, *Appl. Chem. Eng.*, 2024, **7**, 2084.

5 P. Chowdhury, N. A. Mahi, R. Yeassin, N.-U.-R. Chowdhury and O. Farrok, *Energy Convers. Manage.:X*, 2025, **25**, 100889.

6 A. Saravanan, Y. P. Ragini, S. Karishma, R. V. Hemavathy and M. Jyotsna, *Sustain. Futures*, 2025, **10**, 100835.

7 B.-J. R. Mungyeko Bisulandu and F. Huchet, *Appl. Therm. Eng.*, 2023, **221**, 119637.

8 S. Wang and Y. Shen, *Prog. Energy Combust. Sci.*, 2025, **109**, 101221.

9 K. F. Adoko, P. D. Kombienou, H. A. Azontondé and W. Cornelis, *Biomass Bioenergy*, 2026, **206**, 108666.

10 S. Kakku, N. Jonna, A. G. Chakinala, J. Joshi, R. Vinu, C. Thota and A. Sharma, *Ind. Eng. Chem. Res.*, 2024, **63**, 21816–21830.

11 S. Kakku, S. Naidu, M. Bhatt, A. G. Chakinala, J. Joshi, S. Gautam, K. Mohanty, G. Kataria and A. Sharma, *J. Anal. Appl. Pyrolysis*, 2023, **171**, 105951.

12 K. Moser, E. Wopienka, C. Pfeifer, M. Schwarz, I. Sedlmayer and W. Haslinger, *J. Anal. Appl. Pyrolysis*, 2023, **174**, 106112.

13 K. N. Yogalakshmi, T. Poornima Devi, P. Sivashanmugam, S. Kavitha, R. Yukesh Kannah, S. Varjani, S. AdishKumar, G. Kumar and J. Rajesh Banu, *Chemosphere*, 2022, **286**, 131824.

14 P. Singh, T. P. Singh, R. K. Sharma, Y. K. Negi and R. Pal, *J. Agric. Eng.*, 2021, **58**, DOI: 10.52151/jae2021581.1745.

15 S. C. Arya and N. Sijwali, *Int. J. Environ. Sci.*, 2022, **11**(4), 140–144.

16 P. Nain, *Ann. Plant Soil Res.*, 2023, **25**, 211–220.

17 L. D. Kala and P. M. V. Subbarao, *Renewable Energy*, 2018, **128**, 9–19.

18 P. K. Gupta, A. Thakur, S. Gupta, N. Bala, V. Rana, G. Joshi and R. Prakash, *Waste Management Bulletin*, 2024, **2**(2), 140–152.

19 R. Kumar, A. Verma, A. Shome, R. Sinha, S. Sinha, P. K. Jha, R. Kumar, P. Kumar, Shubham, S. Das, P. Sharma and P. V. Vara Prasad, *Sustainability*, 2021, **13**, 9963.

20 P. Das and A. Ganesh, *Biomass Bioenergy*, 2003, **25**, 113–117.

21 S. K. Sanjeeva, M. P. Pinto, M. M. Narayanan, G. M. Kini, C. B. Nair, P. V. SubbaRao, P. K. Pullela, S. Ramamoorthy and C. J. Barrow, *Renewable Energy*, 2014, **71**, 81–88.

22 A. Al-Rumaihi, M. Shahbaz, G. Mckay, H. Mackey and T. Al-Ansari, *Renewable Sustainable Energy Rev.*, 2022, **167**, 112715.

23 J. Hao, F. Xu, D. Yang, B. Wang, Y. Qiao and Y. Tian, *Renewable Sustainable Energy Rev.*, 2025, **208**, 115090.

24 H. Huang, J. Liu, H. Liu, F. Evrendilek and M. Buyukada, *Energy Convers. Manage.*, 2020, **207**, 112552.

25 A. K. Varma and P. Mondal, *J. Therm. Anal. Calorim.*, 2018, **131**(3), 2057–2071.

26 R. K. Mishra, K. Mohanty and X. Wang, *Environ. Prog. Sustainable Energy*, 2024, **43**(3), DOI: 10.1002/ep.14357.

27 R. Kaur, A. Kumar, B. Biswas, B. B. Krishna, P. K. Rout and T. Bhaskar, *Biomass Convers. Biorefin.*, 2024, **14**, 5319–5330.

28 J. J. Manyà, *Environ. Sci. Technol.*, 2012, **46**, 7939–7954.

29 R. K. Mishra, V. Kumar and K. Mohanty, *J. Energy Inst.*, 2020, **93**, 1148–1162.

30 Q. Van Nguyen, Y. S. Choi, S. K. Choi, Y. W. Jeong and Y. S. Kwon, *J. Environ. Manage.*, 2019, **237**, 24–29.

31 A. K. Varma, L. S. Thakur, R. Shankar and P. Mondal, *Waste Manage.*, 2019, **89**, 224–235.

32 A. A. Saleh, *Renewable Energy*, 2018, **124**, 197–201.

33 K. K. B. Suresh Babu, M. Nataraj, M. Tayappa, Y. Vyas, R. K. Mishra and B. Acharya, *Mater. Sci. Energy Technol.*, 2024, **7**, 318–334.

34 A. K. Varma and P. Mondal, *J. Therm. Anal. Calorim.*, 2016, **124**, 487–497.

35 B. Cagnon, X. Py, A. Guillot, F. Stoeckli and G. Chambat, *Bioresour. Technol.*, 2009, **100**, 292–298.

36 S. Kakku, S. Naidu, A. G. Chakinala, J. Joshi, C. Thota, P. Maity and A. Sharma, *Renewable Energy*, 2024, **224**, 120182.

37 A. M. Yahya, A. A. Adeleke, P. Nzerem, P. P. Ikubanni, S. Ayuba, H. A. Rasheed, A. Gimba, I. Okafor, J. A. Okolie and P. Paramasivam, *ACS Omega*, 2023, **8**, 43771–43791.

38 S. Kakku, N. Jonna, A. G. Chakinala, J. Joshi, R. Vinu, C. Thota and A. Sharma, *Ind. Eng. Chem. Res.*, 2024, **63**, 21816–21830.

39 S. Kakku, S. Naidu, M. Bhatt, A. G. Chakinala, J. Joshi, S. Gautam, K. Mohanty, G. Kataria and A. Sharma, *J. Anal. Appl. Pyrolysis*, 2023, **171**, 105951.

40 Y. Huang, D. T. Sekyere, J. Zhang and Y. Tian, *J. Anal. Appl. Pyrolysis*, 2023, **170**, 105922.

41 A. K. Varma and P. Mondal, *J. Energy Resour. Technol.*, 2016, **138**(5), 052205.

42 S. K. Kyei, W. I. Eke, R. D. Nagre, I. Mensah and O. Akaranta, *Cleaner Waste Systems*, 2023, **6**, 100116.

43 E. Apaydın Varol and Ü. Mutlu, *Energies*, 2023, **16**, 3674.

44 E. M. de Paiva, A. L. A. Mattos, G. S. da Silva, K. M. Canuto, R. C. Leitão, J. L. F. Alves and E. S. de Brito, *Ind. Crops Prod.*, 2024, **212**, 118379.

45 P. Das, T. Sreelatha and A. Ganesh, *Biomass Bioenergy*, 2004, **27**, 265–275.

46 S. Mandal, T. K. Bhattacharya, A. K. Verma and J. Haydary, *Chem. Pap.*, 2018, **72**, 603–616.

47 A. Mohan and K. Engvall, *Fuel*, 2026, **406**, 136845.

48 R. Waitongkham, Y. Pianroj, T. Punvichai, S. Karrila, P. Chumkaew and S. Jumrat, *Green Process. Synth.*, 2023, **12**(1), DOI: 10.1515/gps-2023-0084.

49 R. Kaur, V. Tarun Kumar, B. B. Krishna and T. Bhaskar, *Bioresour. Technol.*, 2023, **376**, 128859.

50 P. Das and A. Ganesh, *Biomass Bioenergy*, 2003, **25**, 113–117.

51 S. S. Nagaraja, A. B. Sahu, S. Panigrahy and H. J. Curran, *Combust. Flame*, 2021, **233**, 111579.

52 R. K. Mishra, D. Jaya Prasanna Kumar, R. Sankannavar, P. Binnal and K. Mohanty, *Fuel*, 2024, **360**, 130473.

53 V. Sharma, R. K. Sharma, R. K. A. Razak, D. Thakur, Z. Said, M. Alwetaishi, C. A. Saleel and A. Afzal, *J. Therm. Anal. Calorim.*, 2022, **147**, 12595–12615.

54 C. Sindhuwati, M. A. Nahil and P. T. Williams, *Biomass Bioenergy*, 2026, **204**, 108456.

55 M. Altarawneh and L. Ali, *Energy Fuels*, 2024, **38**, 21735–21792.

56 H. Ravindran, S. Thangalazhy-Gopakumar and S. Adhikari, *Energy Sources, Part A*, 2015, **37**(7), 750–757.

57 R. K. Sharma, J. Haydary, T. P. Singh, M. A. Nazari, S. Mandal and A. Verma, *Biomass Convers. Biorefin.*, 2025, **15**, 12429–12440.

58 A. K. Varma and P. Mondal, *J. Therm. Anal. Calorim.*, 2018, **131**, 2057–2072.

59 S. K. Kyei, W. I. Eke, R. D. Nagre, I. Mensah and O. Akaranta, *Cleaner Waste Systems*, 2023, **6**, 100116.

60 M. L. Adekanbi and T. T. Olugasa, *Cleaner Chemical Engineering*, 2022, **4**, 100085.

61 M. M. Hasan, M. G. Rasul, M. I. Jahirul and M. M. K. Khan, *Energy Convers. Manage.*, 2023, **278**, 116723.

62 A. K. Varma and P. Mondal, *J. Therm. Anal. Calorim.*, 2018, **131**, 2057–2072.

63 A. A. Bamgbola, O. O. Adeyemi, O. O. Olubomehin, A. K. Akinlabi, O. S. Sojinu and P. O. Iwuchukwu, *Curr. Res. Green Sustainable Chem.*, 2020, **3**, 100032.